# MARINE ENVIRONMENTAL EFFECTS ON THE BENDING CREEP OF ANGLE-PLY LAMINATED COMPOSITES

Maozhou Meng[1], Huirong Le[2] and Stephen Grove[3]

[1] Department of Mechanical Engineering and Built Environment, College of Engineering and Technology, University of Derby, UK, http://maozhou.tk
[2] Department of Mechanical Engineering and Built Environment, College of Engineering and Technology, University of Derby, UK, https://www.derby.ac.uk/staff/huirong-le
[3] School of Engineering, Plymouth University, Plymouth, UK, https://www.plymouth.ac.uk/staff/stephen-grove

**Keywords:** Laminated composites, Creep, Moisture diffusion, Finite element analysis

## ABSTRACT

This paper investigates the bending creep of carbon fibre reinforced plastic composites (CFRP) correlating with environmental effects. The study is closely linked to the application of composites in marine renewable energy devices and aircrafts. Composite structures served in marine environment and aerospace are subjected to many aspects in which this paper pursues the effects of water ingress on the creep behaviour. The hygrothermal expansion of the matrix can be induced by the change of moisture content after water immersion, which not only affects the stress distribution in CFRP composites but also degrades the interface of fibre/matrix. Therefore, an accelerated testing method, which includes moisture diffusion and environmental creep, was developed to investigate the interaction between composite creep and marine environmental effects. Angle-ply ([±45]4s) carbon fibre reinforced epoxy composite coupons were designed and manufactured in autoclave, and then submerged in both fresh and seawater for various periods. Bending creep tests were carried out in both air and simulated moisture environment, and the failure mechanisms were investigated using visual and microscopic methods. Additionally, a 3D FEA model was developed to evaluate the stress distribution and the failure mechanisms. The experimental observations gave a good agreement with the FEA solution. The study shows that the creep stiffness was perfectly governed by the power law, and the obvious matrix hardening was observed after water immersion.

## 1 INTRODUCTION

Compared with the aerospace industry, where high strength and stiffness to weight is essential, the use of marine composites was driven by their superior performance of environmental resistance and fatigue life. The growth of the shipment of marine composites has benefited from the development of marine renewable energy and the offshore platforms. Since FRP composites can be moulded to very complex shapes, FRP composites have been used for critical marine structures, such as propellers [1], ship hulls [2], shafts [3], pipes & tanks [4, 5].

Composite structures served in marine environment are subjected to many aspects, such as the long exposure time to moisture, temperature, numerous ionic species as well as microorganisms. The hygrothermal expansion can be developed by the change of moisture content after water immersion, which not only affects the stress distribution in FRP composites but also degrades the interface of fibre/matrix. Therefore, the loss in the mechanical properties of composite materials is mainly attributed to the plasticisation of polymeric matrix. On the other hand, the rate of capillary climb is one million times faster comparing with the moisture diffusivity in polymeric composites, thus the capillary climbing also plays an important role on the creep behaviour while immersed.

Creep is also known as static fatigue, or stress corrosion. According to the open literature, the unidirectional ($[0]_n$) and cross-ply ($[0/90]_n$) laminates have no creep, therefore the angle-ply layup ($[\pm45]_n$) was found in the composite structures combining with unidirectional plies whereas tensile loads were carried by the unidirectional plies, the shear loads were withstood by angle-ply layers literature [6, 7]. Considerable research had been carried out to investigate the marine environmental

effects on either mechanical property, i.e. uniaxial tensile strength/modulus or chemical properties, i.e. moisture diffusion of FRP composites. However, there is still a lack of knowledge on the fracture mechanics of FRP composites when water ingress is considered which is essential to composite failure since the water ingress is also a very slow process.

This study is closely linked to the application of carbon fibre reinforced plastic (CFRP) composites in marine renewable energy devices and aircraft. An accelerated testing method, which includes moisture diffusion and environmental creep, was developed to investigate the interaction between composite creep and marine environmental effects. CFRP coupons with specific stacking sequences were designed and manufactured in autoclave, and then submerged in both fresh and seawater until moisture saturation. Quasi-static test and creep test were carried out in both air and simulated marine environment, and the failure mechanisms were investigated using visual and microscopic methods. Additionally, a robust 3D FEA model was developed to investigate the stress distribution and the failure mechanisms of the bending creep.

## 2 EXPERIMENTAL SETUP

High strength carbon fibre/epoxy pre-preg (Cytec 977-2- 12kHTS) was used in this study. The pre-preg tape was designed as a symmetric angle-ply layup ($[\pm 45]_{4s}$) which was auto-clave manufactured. This is a high temperature (180°C) curing toughened epoxy resin with 212°C glass transition temperature (Tg) which is formulated for autoclave moulding [8]. The manufacturing process and inspection of the defects had been presented in the authors' previous publication [9].

The as-received coupons were first submerged into three chambers which contained fresh water (tap water), sea water and sea water with 70bar hydrostatic pressure. In order to accelerate the procedure of water ingress, all the three chambers were displaced in an oven which maintained 50°C constant temperature. According to the ASTM standard [10], the coupons were moisture saturation after 3-month immersion. The polymer based composites showed a variety of mechanical behaviour before and after water immersion. The experimental results, including diffusion, flexural strength, flexural modulus and interlaminar shear strength had been presented in the authors' previous publication [11]. It was found that the interlaminar shear strength of angle-ply laminate showed very tiny fluctuation between dry condition and time domain water immersion (including the three kinds of water immersion, tested after 1-month and 3-month immersion).

The creep test was carried out on a universal INSTRON machine at room temperature, conducted by ISO standard [12]. Figure 1 gives a snapshot of the angle-ply specimen mounted on the INSTRON machine for the creep test.

**Figure 1. 3-point bending creep test for the angle-ply laminate**

The ISO standard [12] suggests a relation between the span and the specimen thickness,

$$L = (16 \pm 1)h \tag{1}$$

In fact, the ASTM standard [13] also suggests this relation for the flexural test of FRP composites, additionally the ASTM standard recommends 13mm for the width of specimen which was adopted in the present work. The average thickness of the angle-ply laminates for the creep test was 1.95mm, which was the same as those used for diffusion test. Therefore, the 3-point bending span was defined as 32mm and the angle-ply laminate was sliced into dimension of $Length \times Width = 40mm \times 13mm$.

Based on the CLT calculation [9], the flexural modulus of angle-ply laminate $[\pm 45]_{4s}$ was calculated as 16GPa, which was a reference to define the loading level of the creep test. The quasi-static 3-point bending test was carried out to investigate the specimen behaviour prior to the creep test, using the same specimen dimension. The typical relation between deflection and flexural force is plotted in Figure 2.

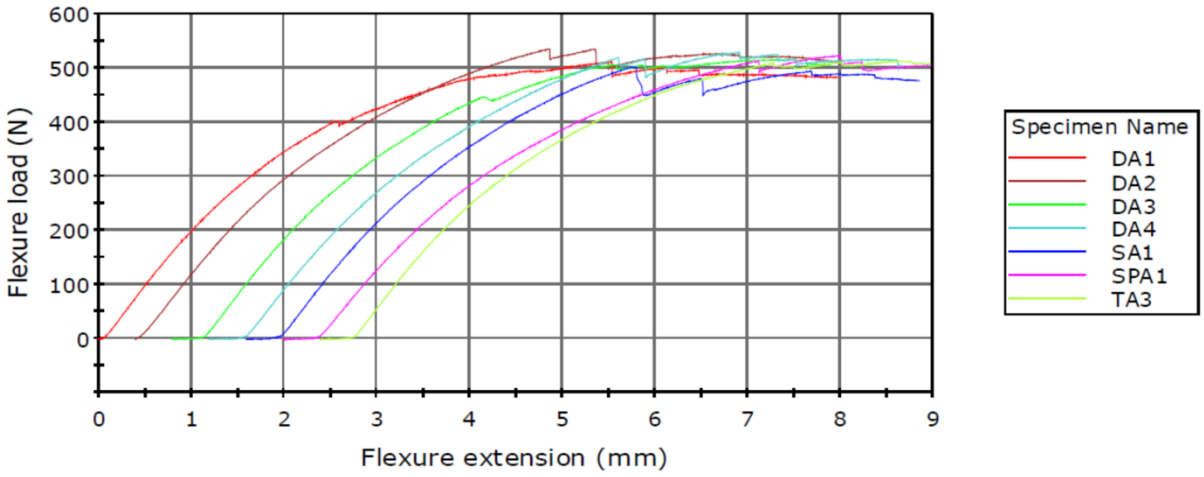


**Figure 2. The loading curves of the angle-ply laminates in quasi-static 3-point bending test. DA: angle-ply laminate without immersion; SA: sea water immersion; SPA: sea water immersion with 70bar hydrostatic pressure; TA: tap water immersion. The 'DA1' specimen was tested at 1mm/min strain rate, while all the others were at 2mm/min.**

As can be seen from the figure, the loading curves were nonlinear and dependent on the loading sequence, i.e. the strain rate. The specimen 'DA1', who was tested at a relatively lower strain rate 1mm/min, presented a relatively smooth parabolic curve without obvious stiffness reduction at the maximum loading point. This is quite different from the others who were tested at 2mm/min shown in the same figure. Moreover there was no linear stage to calculate the flexural modulus. However, no obvious difference was found among the four specimen conditions, i.e. dry, tap water immersion, sea water immersion and sea water immersion with 70 bar hydrostatic pressure.

Compared with the chemical reaction control crack growth which dominates the creep deformation at low loading level, the water immersion of corrosive distance governs the failure process under higher loading level [14]. The apparent yield strength was estimated in the order of 500N and no stiffness loss was found under 400N according to Figure 2, therefore three loading levels were applied for the creep test: 200N, 300N and 400N, corresponding to 194MPa, 291MPa and 388MPa with the given specimen dimension. A ramp rate of 100N/min (approximate 0.5mm/min) was applied until the pre-defined loading level, after that the loading cell was held at a constant force and the deflection was

recoded every 5 seconds. At each loading level, only one specimen corresponding to the immersion condition (dry, tap water and sea water immersions) was tested.

## 3 MODEL DEFINITION

A comprehensive study of bending creep was conducted using commercial FEA code (ABAQUS/STANDARD). Thought the angle-ply laminate is symmetric in geometry and boundary condition, it is asymmetric in material properties. Therefore, a full 3D solid model is required for this study. Figure 3 shows the discretisation of the FEA model. According to the previous report [9], the solution became mesh independent when each ply was divided by three elements through thickness. In order to capture the stress distribution, such as the contact between roll rod and laminate, the mesh at critical region had been refined.

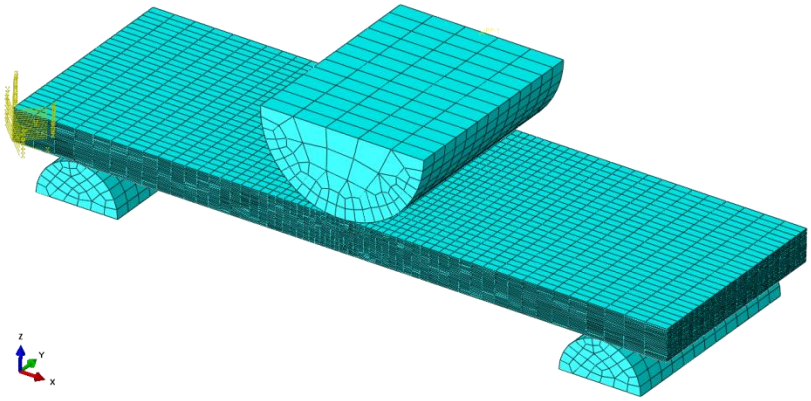

**Figure 3. Mesh plot of the 3D solid FEA model**

The definition of the FEA model was the same as the experimental condition. Individual coordinate systems were created for each plies. Table 1 gives the material properties of the FEA model.

**Table 1 Material properties of lamina**

| **Symbol** | $E_1$ (GPa) | $E_2 = E_3$ (GPa) | $G_{12} = G_{13}$ (GPa) | $G_{23}$ (GPa) | $\nu_{12} = \nu_{13}$ | $\nu_{23}$ |
|---|---|---|---|---|---|---|
| **Value** | 139 | 8.8 | 4.7 | 3.0 | 0.26 | 0.48 |

## 4 RESULTS AND DISCUSSION

### 4.1 Flexural modulus

The typical loading curve of an angle-ply specimen at 300N level at the ramp stage is plotted in Figure 4, showing a good linear relation between the flexural force and deflection. The apparent flexural modulus was a fraction lower than the CLT prediction, in which one possible reason is because of the short span in the 3-point bending.

Table 2 gives an overview of the flexural modulus of different immersion conditions various to the three loading levels. As can be seen from the table, at the same loading level, the flexural modulus extracted from the linear stage provided relatively lower value for the dry specimen than those of the other immersions, which is quite similar with the matrix dominated laminate (i.e. UT $[90]_{16}$ laminate). One possible reason is that the matrix became stiffer after the water immersion. However, the

information shown in the table cannot provide sufficient evidence to distinguish the effects of the three types of water immersions on the apparent flexural modulus.

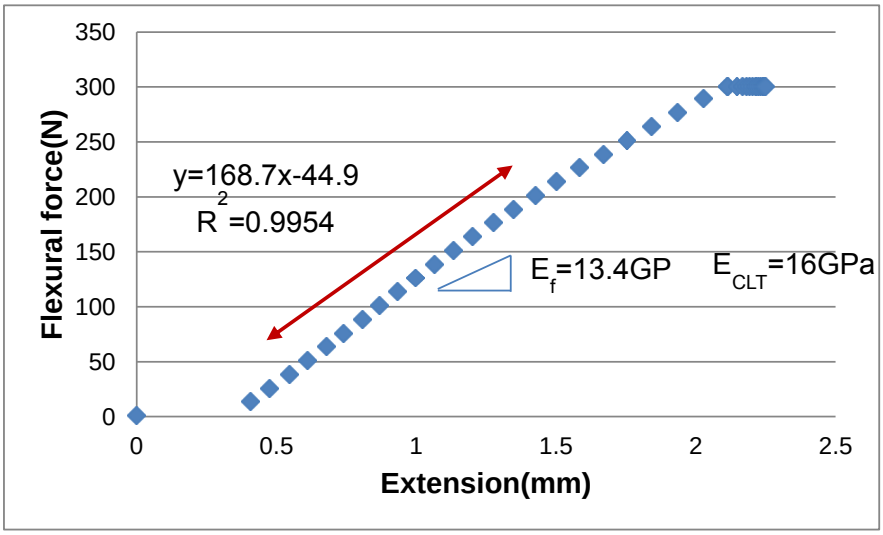


**Figure 4. A typical loading curve of an angle-ply specimen in 3-point bending creep test at the increasingly loading stage, showing good linear relationship**

**Table 2 Flexural modulus of angle-ply laminate at different loading level and immersions**

| | 200N | 300N | 400N |
|---|---|---|---|
| AP-dry | 13.4GPa | 13.4GPa | 13.6GPa |
| AP-sea | 14.2GPa | 13.4GPa | 14.1GPa |
| AP-SP | 14.0GPa | 13.7GPa | 14.2GPa |
| AP-tap | 14.3GPa | 13.1GPa | 14.3GPa |

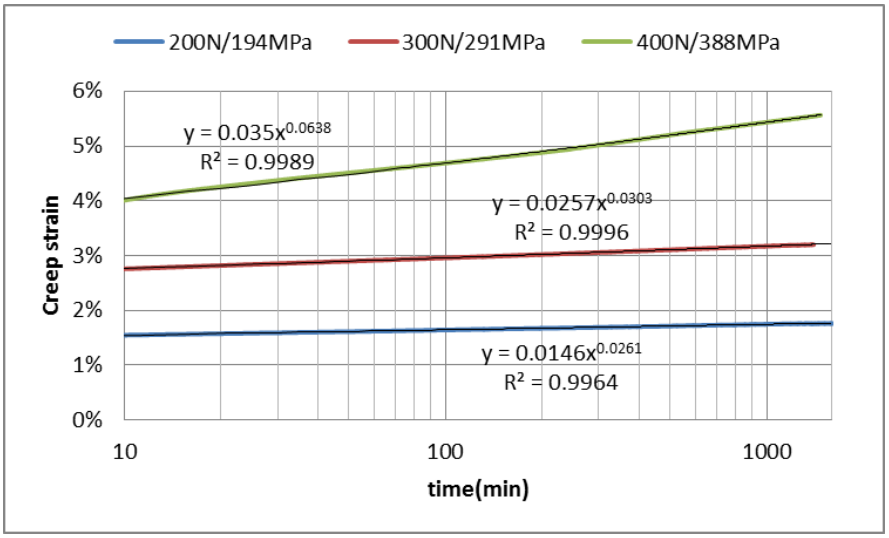


**Figure 5. Typical deflection curve of an angle-ply specimen in 3-point bending creep test at the creep deformation stage, showing a perfect power law relation in time domain. The power law fitting results are also shown in the figure.**

Figure 5 shows the typical deflection curves of angle-ply specimen at the creep deformation stage. The creep strain was plotted against the logarithm of the time under loading level. It can be seen from the figure that the creep deformation was perfectly governed by power law.

### 4.2 Creep stiffness

In Figure 4, it had been shown that the flexural force was linear to the deflection at the increasingly loading stage and later on the deflection was exponential to the creep time at the constant loading stage. Due to the relative short span, the flexural modulus extracted from the increasingly loading stage showed relatively high deviation. The apparent flexural modulus was also highly dependent on the strain rate. The flexural force was linear to the deflection in case of very low strain rate, i.e. 0.5mm/min. Therefore, the creep behaviour of the angle-ply laminate is to be investigated by both the creep strain and stiffness.

According to the ISO standard [12], the creep strain and creep stiffness (flexural-creep modulus) can be calculated by,

$$\begin{aligned} \varepsilon_t &= \frac{6D_t h}{L^2} \\ E_t &= \frac{L^3 F}{4wh^3 D_t} \end{aligned} \tag{2}$$

where $D_t$ is the deflection at the loading point at time t; w and h are the width and thickness of the specimen respectively; F is the applied force; and L is the span. The equation has no terms to represent the creep deformation at the increasingly loading stage. Nutting [15] proposed a more general function which includes the terms of loading level and the deformation at both the increasingly loading stage and constant loading stage (creep deformation),

$$\varepsilon(\sigma,t) = \varepsilon_0(\sigma,t) + \varepsilon_t(\sigma,t) \tag{3}$$

In case of very slow strain rate and proper stress level, for example 0.5mm/min and 388MPa (the yield stress was approximate 486MPa) in this study, the first terms of the equation $\varepsilon_0(\sigma)$ is linear to the loading time. The second terms $\varepsilon_t(\sigma)$ should contain an exponential expression. Nutting proposed an empirical expression for the second terms,

$$\varepsilon_t(\sigma,t) = K\sigma^m t^n \tag{4}$$

According to the experimental observation [16], the exponential parameter of time is independent of the temperature.

Therefore, equation (3) has a form like,

$$\varepsilon(\sigma,t) = \begin{cases} C_1 t, t \le F/R_F \\ C_2 \sigma^{C_3} t^{C_4}, t > F/R_F \end{cases} \tag{5}$$

where $C_1$, $C_2$, $C_3$ and $C_4$, are the material properties, $F, R_F$ are the target loading level in N and the loading rate in N/min.

The first parameter $C_1$ can be fitted by the relation of the strains at the four loading levels (0N, 200N, 300N and 400N), while the others was fitted by MATLAB toolbox 'CFTOOL'. For the fitting of the three parameters of the exponential terms, the fitting tool returned a value with small deviation for the last parameter $C_4$ at different loading levels; however the other parameters showed competition

at different loading levels. Therefore, the value fitted from the intermediate loading level (300N, 291MPa) was used to represent the corresponding immersion condition. Table 3 lists the fitting results of the four parameters for the four immersions.

**Table 3 Fitting results of the four parameters for equation (5). The R square is also given in the table (the unit of stress: MPa; time: minute).**

| | $C_1$ | $C_2$ | $C_3$ | $C_4$ | $R^2$ |
|---|---|---|---|---|---|
| Dry | 0.0089 | 0.0017 | 0.48 | 0.03 | 0.9996 |
| Sea | 0.0081 | 0.002 | 0.45 | 0.029 | 0.9987 |
| SP | 0.0083 | 0.0017 | 0.45 | 0.03 | 0.9936 |
| Tap | 0.0081 | 0.002 | 0.43 | 0.04 | 0.9995 |

After the water immersion, the specimen became stiffer and the maximum deflection of dry specimen was higher than those of water immersions, which had been discussed in the previous section. It has been known that the viscoelastic response of epoxy and epoxy composites is strongly coupled with the moisture content [17-19], however there was no obvious evidence summarized to identify the effects of water immersion on the creep deformation according to the four parameters shown in Table 3. One possible reason is that those immersion specimens were not wetted by a sponge during the creep test. This is similar with the phenomenon observed from the fatigue test, which suggests that the effects of water immersion on the creep deformation are more likely to be an inversely physical process in short time of exposure rather than chemical process. Kibler's research [20], which showed similar results, reported that the creep compliance of AS/3502 $[\pm 45]_{2s}$ specimen showed only a tiny fluctuation in different levels of humidity but a huge shift due to the elevated temperature. At the meantime, the degradation of fibre/matrix interphase from SEM study [11] indicates the creep response might be different in long time of exposure.

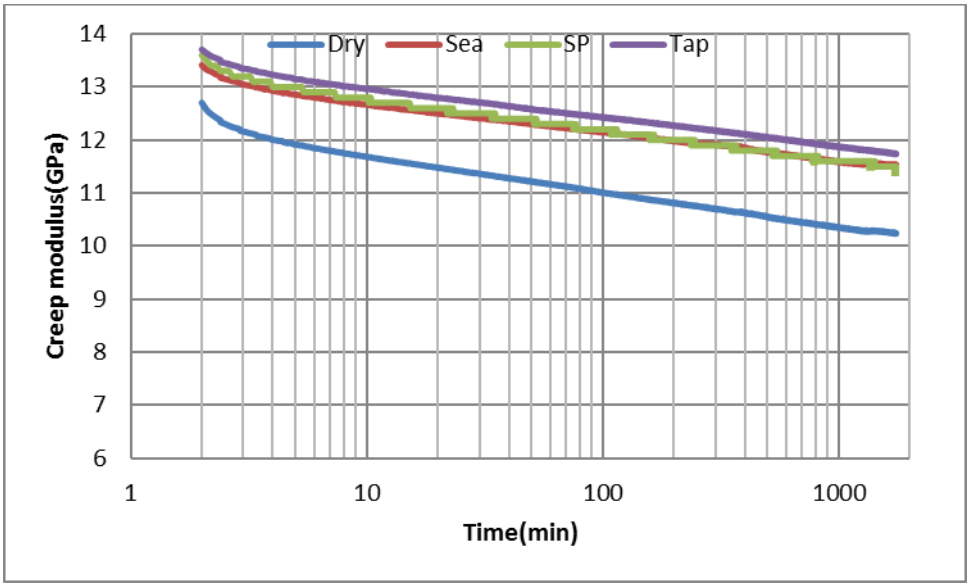


**Figure 6. Creep stiffness of AP specimen at 200N**

Figure 6-8 show the creep stiffness of the angle-ply laminate in the four immersion conditions at 200N, 300N and 400N loading levels respectively. Since the same loading rate, 100N/min was applied for all specimens; the time of the increasingly loading stages were 2, 3 and 4 minutes for the three cases corresponding to the different onset of the creep deformation shown in the figures. The common characteristics can be seen from the three figures that specimen became stiffer after water immersion and the creep stiffness curves plotted in the three figures suggest a power law for the history.

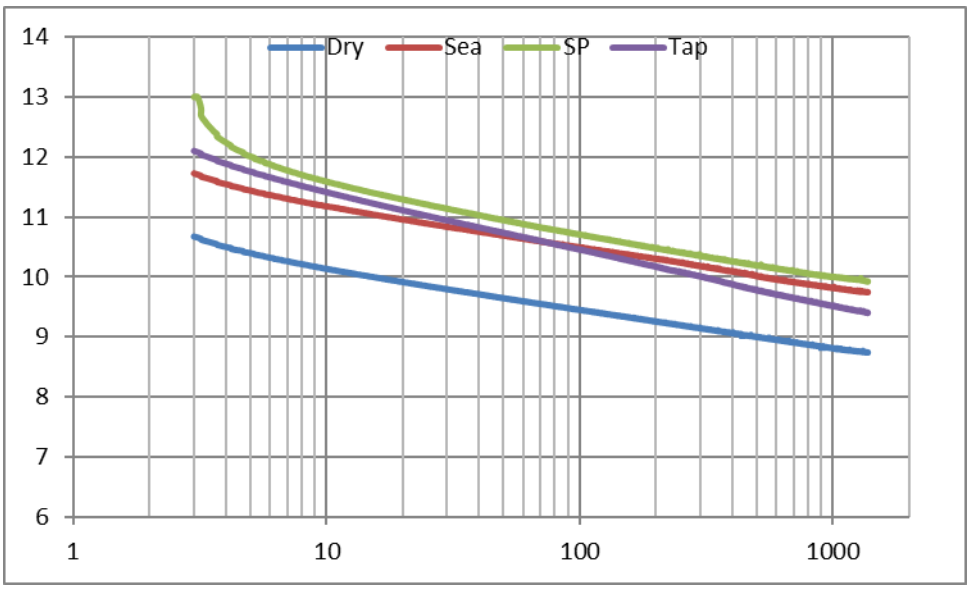


**Figure 7. Creep stiffness of AP specimen at 300N**

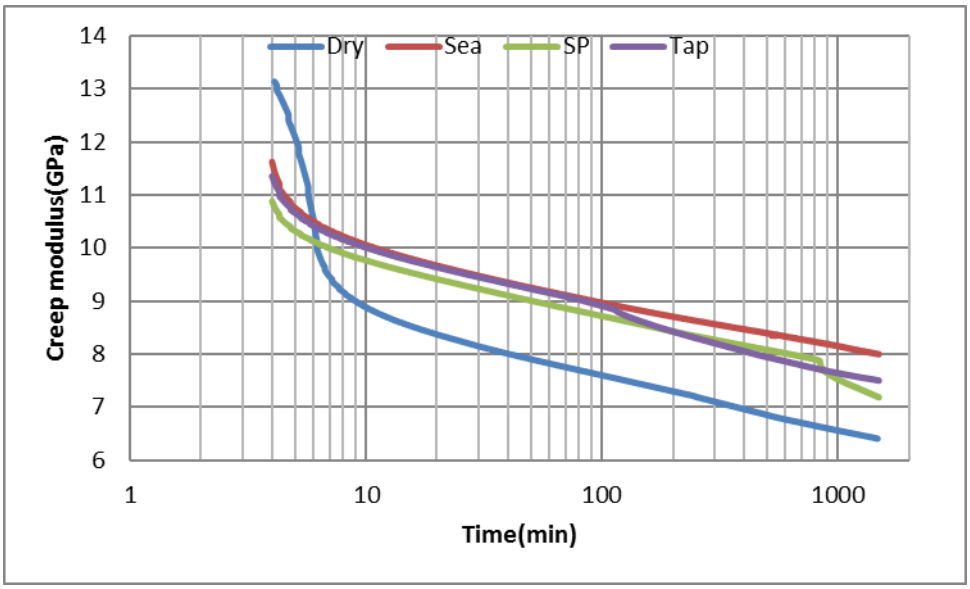


**Figure 8. Creep stiffness of AP specimen at 400N**

### 4.3 Stress distribution

In the quasi-static 3-point bending test, an unidentified failure mode was observed, as shown in Figure 9. Periodic fibre break can be found to be parallel to the load cell at the contact area on the compressive surface.

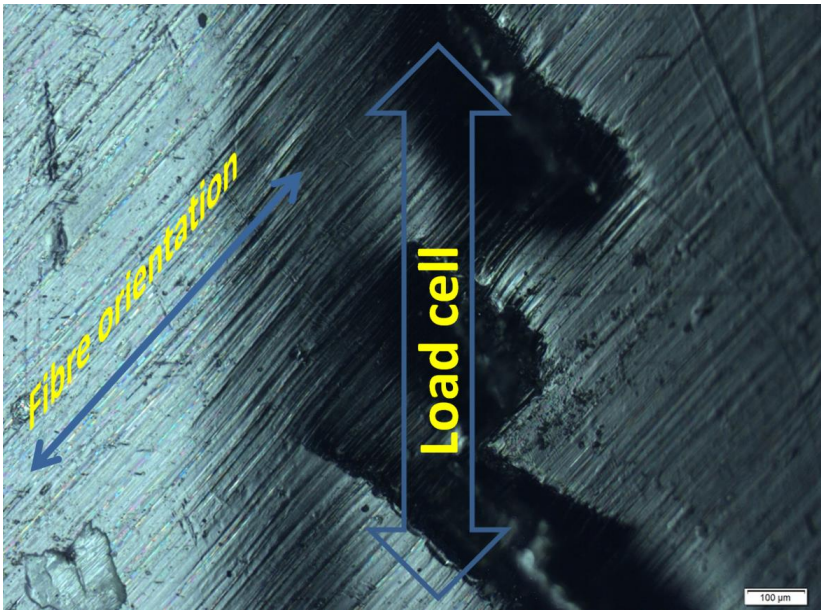


**Figure 9a. A typical failure image of angle-ply specimen in 3-point bending quasi-static test**

As can be estimated from the figure, the periodic distance of this fibre break was in range of 200-300µm. One possible reason is the surface ply failed by in-plane shear stress which was induced by the compressive stress due to the nature of bending, since the maximum compressive stress appears at the top surface. According to the CLT formulation, the interaction ratio $\eta_{xyx}$ of the angle-ply laminate $[\pm 45]_{4s}$ can be calculated as -0.5, which means that the in-plane shear strain $\gamma_{xy}$ induced by the normal stress $\sigma_x$ can be as high as half of the normal strain $\varepsilon_x$.

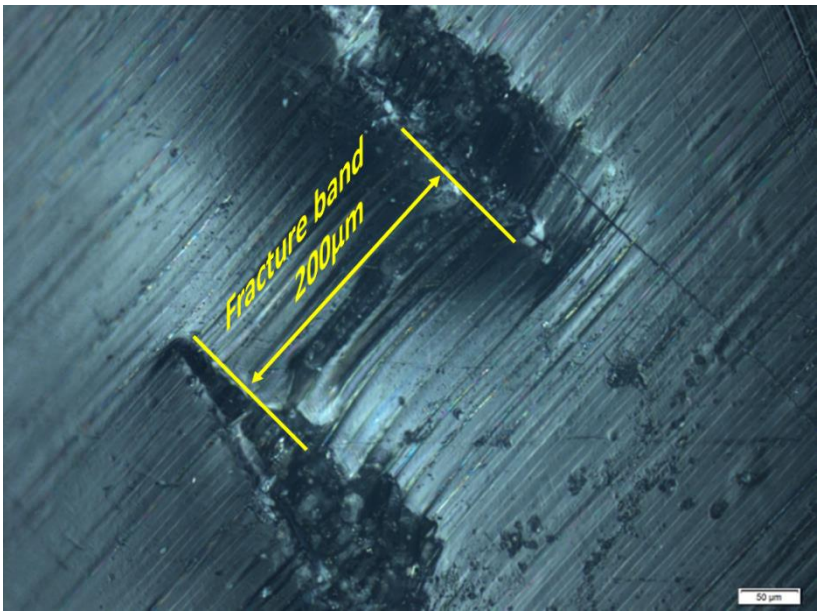


**Figure 9b. The band width of fibre fracture on the top surface of angle-ply specimen in 3-point bending quasi-static test**

It should be noted that these periodic fibre fracture were only found at the centre of top surface underneath the loading cell, where maximum contact pressure applied. Figure 10 shows the distribution of contact pressure of the angle-ply laminate in quasi-static 3-point bending.

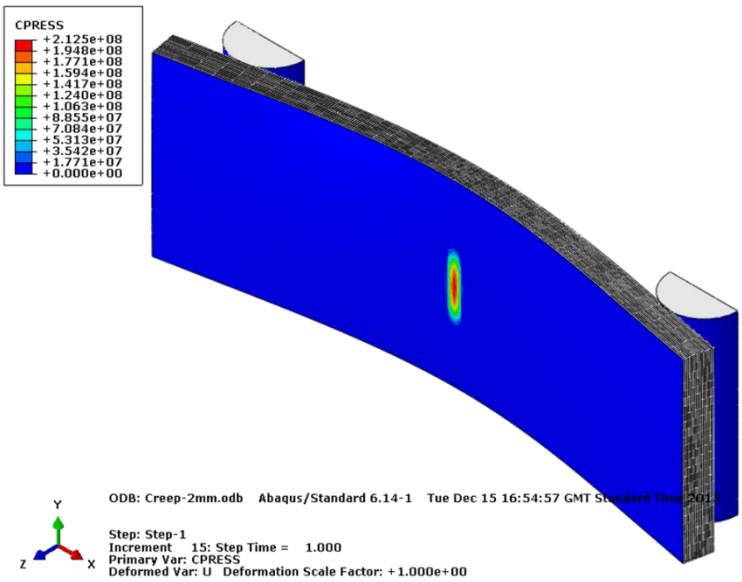


**Figure 10. The contact pressure of angle-ply laminate in quasi-static 3-point bending**

From Figure 10, the maximum contact pressure is in the order of 200 MPa, which is considerably lower than the longitudinal tensile or compressive strength of the laminate, however this value is comparable to the shear strength. Therefore, the failure mechanism of the angle-ply is likely to be associateed with the other stress components. Figure 11-12 shows the distribution of in-plane shear stress and interlaminar shear stress of the angle-ply laminate in quasi-static 3-point bending.

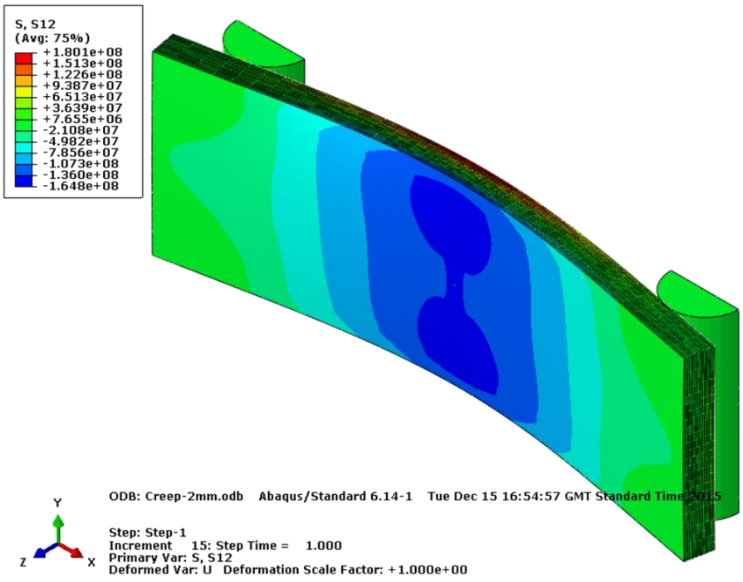


**Figure 11. Distribution of in-plane shear stress of angle-ply laminate in 3-point bending**


**Figure 12. Distribution of interlaminar shear stress of angle-ply laminate in 3-point bending**

It can be seen from Figure 11-12 that the maximum interlaminar shear stress appears near the mid plane of the laminate and the maximum value is considerably lower than the interlaminar shear strength (about 100 MPa), however, the in-plane shear stress has exceeded the strength. Moreover, the maximum in-plane shear stress appears at the surface plies, which combines with the contact pressure leading to the periodic fibre fracture on the top surface.

## 5 CONCLUSIONS

The environmental effects on the creep behaviour of angle-ply composite laminates have been studied by the experiment and FEA modelling. The study of creep test showed that the matrix hardened after water immersion: immersed coupons presented higher creep stiffness compared to the dry specimen at all the three loading levels. It was found that the relation between creep strain and creep time was perfectly governed by power law, and a semi-empiric 4-paremeter model was proposed to describe this relation. However, no evidence was found to identify the different effects of the three immersions on the creep performance.

An unidentified failure mode was found at the top surface of angle-ply laminate underneath the loading cell from the 3-point bending creep test. FEA modelling showed that this periodic fibre fracture was probably induced by the combination of contact pressure by the loading cell and the in-plane shear stress. There is no current mathematical model to predict the band width of this periodic fracture, therefore further study should be carried out to investigate this failure mode.

## REFERENCES

[1] G. Marsh, "A new start for marine propellers?," *Reinforced Plastics*, vol. 48, pp. 34-38, 2004.

[2] D. Hull and T. Clyne, *An introduction to composite materials*: Cambridge university press, 1996.

[3] E. Greene, *Marine composites*: Eric Greene Associates, 1999.

[4] S. Selvaraju and S. Ilaiyavel, "Applications of composites in marine industry," *J. Eng. Res. Stud., II*, pp. 89-91, 2011.

[5] C. Smith, "Design of submersible pressure hulls in composite materials," *Marine structures*, vol. 4, pp. 141-182, 1991.

[6] J. Petermann and K. Schulte, "The effects of creep and fatigue stress ratio on the long-term behaviour of angle-ply CFRP," *Composite Structures*, vol. 57, pp. 205-210, 7// 2002.

[7] J. R. Reeder, K. Song, P. Chunchu, and D. R. Ambur, "Postbuckling and growth of delaminations in composite plates subjected to axial compression," in *The 43rd AIAA/ASME/ASCE/AHS/ASC Structures, Structural Dynamics, and Materials Conference*, 2002.

[8] Cytec, "CYCOM 2237 Polyimide resin system. www.cytec.com," *Technical data sheet*, 2012.

[9] M. Meng, H. R. Le, M. J. Rizvi, and S. M. Grove, "3D FEA modelling of laminated composites in bending and their failure mechanisms," *Composite Structures*, vol. 119, pp. 693-708, 1// 2015.

[10] A. D5229/D5229M, "Standard Test Method for Moisture Absorption Properties and Equilibrium Conditioning of Polymer Matrix Composite Materials," in *ASTM* vol. ASTM D5229, ed, 2004, p. 13.

[11] M. Meng, M. J. Rizvi, S. M. Grove, and H. R. Le, "Effects of hygrothermal stress on the failure of CFRP composites," *Composite Structures*, vol. 133, pp. 1024-1035, 12/1/ 2015.

[12] ISO899-2:2003, "Plastics -- Determination of creep behaviour -- Part 2: Flexural creep by three-point loading," ed, 2003.

[13] A. D7264, "Standard Test Method for Flexural Properties of Polymer Matrix Composite Materials," ed: ASTM International, 2007.

[14] A. Evans, "A method for evaluating the time-dependent failure characteristics of brittle materials—and its application to polycrystalline alumina," *Journal of Materials Science*, vol. 7, pp. 1137-1146, 1972.

[15] P. G. Nutting, "A Study of Elastic Viscous Deformation," *ASTM Proceeding 1921*, vol. 21, p. 10, 1921.

[16] W. N. Findley and F. A. Davis, *Creep and relaxation of nonlinear viscoelastic materials*: Courier Corporation, 2013.

[17] L.-W. Cai and Y. Weitsman, "Non-Fickian moisture diffusion in polymeric composites," *Journal of composite materials*, vol. 28, pp. 130-154, 1994.

[18] Y. Weitsman, "Stress assisted diffusion in elastic and viscoelastic materials," *Journal of the Mechanics and Physics of Solids*, vol. 35, pp. 73-94, 1987.

[19] Y. Weitsman, "Stresses in adhesive joints due to moisture and temperature," *Journal of Composite Materials*, vol. 11, pp. 378-394, 1977.

[20] K. Kibler, "Time-dependent environmental behavior of graphite/epoxy composites," DTIC Document1980.